reduced considerably. We recall that both $|\eta_{00}|$ and $|\eta|$ are directly accessible to experiment:

$$|\eta_{00}|^2=\frac{\Gamma(K_L\to\pi^0\pi^0)}{\Gamma(K_S\to\pi^0\pi^0)}$$

and

$$|\eta|^2=0.986\frac{\Gamma(K_S\to\pi^0\pi^0)}{\Gamma(K_S\to\pi^+\pi^-)},$$

where the numerical factor on the right-hand side is the phase-space correction.

(3) The determination of θ_+, the phase of the amplitude $A_2{}^+=(A^{(3/2)}-A^{(5/2)})/\sqrt{2}$ is a much more difficult task. Recently, it has been suggested by Cline,[38] that θ_+ could, in principle, be obtained from the measurement of the π^+-energy spectrum in $K^+\to\pi^+\pi^0\gamma$ decays. The method, however, needs the *a priori* knowledge of the direct matrix elements, and therefore becomes very much model-dependent. Experiments on $K^\pm\to\pi^\pm\pi^0\gamma$ decays (measurement of decay rates, spectra, and polarizations) are nevertheless very important in the sense that they can lead to the detection of sizeable *CP*-noninvariant effects.[39] A better understanding of these decays could lead, eventually, to the determination of the phase of the $A_2{}^+$ amplitude.

Note added in proof. Recently two values have been obtained for Reϵ by measuring the asymmetry in three-body semileptonic K_L decay [see Eq. (27)]. Ignoring the small $\Delta S=-\Delta Q$ correction term, Dorfan *et al.*[40] find (from $K_L\to\pi\mu\nu$) Re$\epsilon=(2.0\pm0.7)\times10^{-3}$, and Bennett *et al.*[41] find (from $K_L\to\pi e\nu$) Re$\epsilon=(1.11\pm0.18)\times10^{-3}$, both experiments showing that solution *a* is the physical one. However, this solution (see Table II) predicts a value for $(\delta_2-\delta_0)$ which is inconsistent with the evidence from a considerable body of other experiments[37] (even allowing for the fact that $(\delta_2-\delta_0)$ is determined only up to $\pm n\pi$). If one accepts the latter estimates[37] of $(\delta_2-\delta_0)$, then it is likely that the value of at least one of the input parameters in the $K^0-\bar{K}^0$ system is in error. A possible candidate is θ_{+-} whose value has fluctuated considerably in the past. The latest "world-average" value for θ_{+-} is[42] $60°\pm12°$, but the spread on the individual experiments is still considerable.

Using the techniques of Sec. III and the data of Table I[43] we find that[37] $-90°\lesssim(\delta_2-\delta_0)\lesssim0°$ implies $20°\lesssim\theta_{+-}\lesssim55°$, and for this range of θ_{+-}, $1.90\lesssim$ Re$\epsilon\lesssim2.05$. We note that for a value of $\theta_{+-}\sim45°$ a consistent picture emerges for the parameters of $K\to2\pi$ decay provided that Re$\epsilon\simeq2\times10^{-3}$. It is clear that an accurate measurements of θ_{+-} is needed.

ACKNOWLEDGMENT

We wish to thank the members of the Theory Group at Brookhaven for discussions.

[38] D. Cline, Nuovo Cim. **48A**, 566 (1967).

[39] Some of the possible effects have been recently discussed by G. Costa and P. K. Kabir, Phys. Rev. Letters **18**, 429 (1967); S. Barshay, *ibid.* **18**, 515 (1967); and N. Christ, Phys. Rev. **159**, 1292 (1967).

[40] D. Dorfan *et al.*, in Proceedings of the Stanford Conference on Electron and Photon Interactions at High Energies, 1967 (unpublished).

[41] B. Bennett *et al.*, in Proceedings of the Stanford Conference on Electron and Phonon Interactions at High Energies, 1967 (unpublished).

[42] V. L. Fitch, Lectures at the Second Hawaii Topical Conference, 1967 (unpublished).

[43] For $|\eta_{00}|$ we use the most recent value of $|\eta_{00}|=(4.17\pm0.30)\times10^{-3}$ as given by J. W. Cronin [in Proceedings of the Rochester Conference on Elementary Particles and Fields, 1967 (unpublished)].

PHYSICAL REVIEW VOLUME 162, NUMBER 5 25 OCTOBER 1967

Model for Electron Excitation of the Nucleon*

J. D. WALECKA

Institute of Theoretical Physics, Department of Physics, Stanford University, Stanford, California

(Received 21 April 1967)

A very crude model of oscillations of the meson field in the nucleon is made which gives an excitation spectrum similar to that of the nucleon and which allows us to calculate the transition form factors for the allowed normal-parity Coulomb transitions $\frac{1}{2}^+\to\frac{3}{2}^-,\frac{5}{2}^+,\frac{7}{2}^-$, etc. The results are compared with the recent Cambridge Electron Accelerator (CEA) data, and predictions, applicable to the planned Stanford Linear Accelerator (SLAC) experiments, are made for the other relevant isobars and other momentum transfers.

1. INTRODUCTION

THE advent of very high-energy electron accelerators makes electron excitation a practical means of studying the details of the excited states of the nucleon. The well-known $J^\pi=\frac{3}{2}^+$, $T=\frac{3}{2}$ (1236 MeV) resonance has already been studied extensively with existing machines.[1–4] However, the nucleon is now

* Research sponsored by the U. S. Air Force Office of Scientific Research, Office of Aerospace Research, under AFOSR Contract No. AF49(638)-1389. A preliminary version of this work was reported on at the International Conference on Electromagnetic Interactions at Low and Intermediate Energies, Dubna, U.S.S.R., February, 1967 (to be published).

[1] W. K. H. Panofsky and E. Allton, Phys. Rev. **110**, 1155 (1958).

[2] L. N. Hand, Phys. Rev. **129**, 1834 (1963).

[3] H. Lynch, Ph.D. thesis, Stanford University, 1966 (unpublished).

[4] K. Berkelman, International Conference on Electromagnetic Interactions at Low and Intermediate Energy, Dubna, U.S.S.R., 1967 (to be published).

known to have many levels, and an exhaustive study of the higher resonances is planned at the Standard Linear Accelerator Center (SLAC).[5] Some important data on these levels are already available from the Cambridge Electron Accelerator (CEA) group.[6] To indicate the richness of possibilities here we show the "low-lying" spectrum of the nucleon in Fig. 1.[7]

From both a theoretical and an experimental standpoint, one would like to have some idea of what to expect in these experiments. From a theoretical point of view, one would at least like to make some predictions *before* the experiments are carried out, and from an experimental point of view, estimates of the transition form factors are useful in planning new experiments and in interpreting, understanding, and correlating the data as they accumulate.

The detailed theoretical understanding of these higher excited states requires a theory of strong interactions; but reliable, quantitative calculations are exceedingly difficult and in many cases quite impossible at the present time, although the experiments themselves will stimulate work in this area and lead to new ideas here. In this paper we make a model, which by necessity is very crude, which exhibits a level structure quite similar to that shown in Fig. 1, and which allows us to make a calculation of the transition form factors. The results are compared with the existing CEA data, and predictions are made for higher-energy excitations and other momentum transfers. Just by looking at the existing data, it is evident that we have already learned some exciting things about the structure of the nucleon.

2. ELECTRON SCATTERING

We first give a very brief review of the theory of electron scattering. We concentrate on the case where only the final electron is detected, as in most of the experiments which have been done so far and as will be the case in the SLAC experiments.[5] Bjorken and

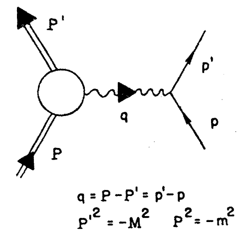

FIG. 2. Kinematics for inelastic electron scattering.

Walecka[8] have given a relativistically covariant analysis of the process of electron excitation of the nucleon and have discussed all that can be said about the transition form factors on general grounds. They also show the relation to photoexcitation of the nucleon resonances. We summarize their results here.

The kinematical situation in the one-photon exchange approximation is shown in Fig. 2. The angular momentum analysis is best carried out in the rest frame of the final isobar, because one then has an eigenstate of angular momentum and parity. The electromagnetic vertex is characterized by four reduced matrix elements, or equivalently by the four linear combinations

$$f_\rho = \left(\frac{EE'\Omega^2}{8\pi M^2}\right)^{1/2} \sum_j \left(\frac{2j+1}{2J+1}\right)^{1/2} (j\tfrac{1}{2}1\rho\,|\,j1J\tfrac{1}{2}+\rho) \times \langle \pi_R J \| \hat{\mathbf{J}}(0) \| q^* \pi j\rangle, \quad (2.1)$$

with $\rho = \pm 1$, 0 and

$$f_c = \left(\frac{EE'\Omega^2}{8\pi M^2}\right)^{1/2} \langle \pi_R J \| \hat{J}_0(0) \| q^* \pi J\rangle. \quad (2.2)$$

In these expressions E and E' are the initial and final target energies, M is the isobar mass, Ω is the normalization volume, $\hat{J}_\mu(0) = (\hat{\mathbf{J}}(0), i\hat{J}_0(0))$ is the electromagnetic current operator taken at the origin, and $J^{\pi R}$ is the angular momentum and parity of the isobar. In the rest frame of the isobar one has

$$q_\mu \equiv (\mathbf{q}^*, iq_0). \quad (2.3)$$

There is still one relation among these four quantities coming from current conservation, and it simply eliminates f_0:

$$f_0 = (q_0/q^*) f_c. \quad (2.4)$$

The electron-scattering cross section in the laboratory is then shown to be (we set $m_e = 0$)

$$\left.\frac{d\sigma}{d\Omega}\right|_{\text{lab}} = \frac{\alpha^2 \cos^2(\frac{1}{2}\theta)}{4\epsilon^2 \sin^4(\frac{1}{2}\theta)[1+(2\epsilon/m)\sin^2(\frac{1}{2}\theta)]} \times \left\{ \frac{q^4}{q^{*4}} |f_c|^2 + (q^2/2q^{*2} + (M^2/m^2)\tan^2(\tfrac{1}{2}\theta)) \times [|f_+|^2 + |f_-|^2] \right\}. \quad (2.5)$$

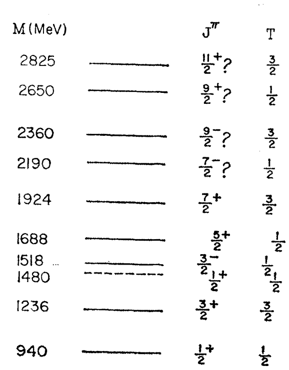

FIG. 1. "Low-lying" spectrum of the nucleon (Ref. 7).

[5] SLAC Group A—Proposal 4B, 1966; W. Panofsky, D. Coward, H. DeStaebler, J. Litt, L. Mo, R. Taylor, J. Friedman, H. Kendall, L. Van Speybroek, C. Peck, and J. Pine (unpublished).

[6] A. Cone, K. W. Chen, J. R. Dunning, Jr., G. Hartwig, N. F. Ramsey, J. K. Walker, and Richard Wilson, Phys. Rev. **156**, 1490 (1967). See also Phys. Rev. Letters **14**, 326 (1965).

[7] A. H. Rosenfeld, A. Barbaro-Galtieri, W. H. Barkas, P. L. Bastien, J. Kirz, and M. Roos, Rev. Mod. Phys. **37**, 633 (1965).

[8] J. D. Bjorken and J. D. Walecka, Ann. Phys. (N. Y.) **38**, 35 (1966).

In this expression ϵ is the initial electron energy, θ is the electron scattering angle, m is the nucleon mass, and $q^2=q_\mu^2$ is the invariant four-momentum transfer. We see that electron scattering measures two independent combinations of form factors, the Coulomb and transverse form factors. These may be separated experimentally by keeping q^2 and the energy loss $-q_0=\epsilon-\epsilon'$ fixed and varying θ or by working at $\theta=180°$, where only the transverse contribution remains. The transverse form factor can also be measured *at one momentum transfer*, namely, $q_\mu^2=0$ or

$$q^*_{\text{threshold}}=(M^2-m^2)/2M\,, \tag{2.6}$$

in photoexcitation

$$\int_{\text{lab; over resonance}} \sigma_\gamma(\omega)d\omega=\frac{4\pi^2\alpha}{M^2-m^2}\frac{M^2}{m}\times[|f_+|^2+|f_-|^2]_{q^2=0}\,. \tag{2.7}$$

Thus, with electron scattering, we can add a whole new dimension to the photon problem. There is also the possibility of direct Coulomb excitation.

Detailed properties of the form factors f_c, $f_\pm$ are highly model-dependent. However, in the limit $q^*\to 0$ (which implies $-q_0\to M-m$), the form factors have simple threshold behaviors:

1. Normal-parity transitions[9] $\frac{1}{2}^+\to\frac{3}{2}^-, \frac{5}{2}^+\cdots$

$$f_c\sim(q^*)^{J-1/2}\,,$$
$$f_\pm\sim(q^*)^{J-3/2}\,.$$

2. Abnormal-parity transitions $\frac{1}{2}^+\to\frac{1}{2}^-, \frac{3}{2}^+, \frac{5}{2}^-\cdots$

$$f_c\sim(q^*)^{J+1/2}\,,$$
$$f_\pm\sim(q^*)^{J-1/2}\,.$$

One of the interesting questions on which we would like our model to shed some light is whether or not these threshold behaviors are of any use, because only space-like momentum transfers are available experimentally $[q^2\geqslant 0]$, and it is not clear whether the threshold behavior still persists there, since this implies a minimum three-momentum transfer

$$q^*\geqslant q^*_{\text{threshold}}=(M^2-m^2)/2M\,.$$

For the normal-parity transitions there is an additional relation between f_c and $f_\pm$ valid near threshold:

$$\frac{|f_+|^2+|f_-|^2}{|f_c|^2}\underset{q^*\to 0}{\approx}\left(\frac{J+\frac{1}{2}}{J-\frac{1}{2}}\right)\left(\frac{q_0}{q^*}\right)^2. \tag{2.8}$$

This relation is well known in nuclear physics.[10] In particular, it is the relation which allows one to get photon lifetimes for electric transitions from Coulomb excitation.

With a well-localized source, as is the case in nuclear physics, one can give expressions for the transition form factors in terms of the Fourier transforms of the transition charge and current densities[10]:

$$|f_c|^2=\frac{4\pi}{2J_i+1}\sum_{L=0}^{\infty}|\langle J_f\|\hat{M}_L{}^{\text{Coul}}(q^*)\|J_i\rangle|^2, \tag{2.9}$$

$$\begin{aligned}
|f_+|^2+|f_-|^2&=\frac{4\pi}{2J_i+1}\sum_{L=1}^{\infty}[|\langle J_f\|\hat{T}_L{}^{\text{el}}(q^*)\|J_i\rangle|^2 \\
&\qquad+|\langle J_f\|\hat{T}_L{}^{\text{mag}}(q^*)\|J_i\rangle|^2],\\
\hat{M}_{LM}{}^{\text{Coul}}(q^*)&=\int j_L(q^*x)Y_{LM}(\Omega_x)\hat{\rho}(\mathbf{x})d\mathbf{x}\,,\\
\hat{T}_{LM}{}^{\text{el}}(q^*)&=\frac{1}{q^*}\int\nabla\times[j_L(q^*x)\mathfrak{Y}_{LL1}{}^M(\Omega_x)]\cdot\hat{\mathbf{J}}(\mathbf{x})d\mathbf{x}\,,\\
\hat{T}_{LM}{}^{\text{mag}}(q^*)&=\int[j_L(q^*x)\mathfrak{Y}_{LL1}{}^M(\Omega_x)]\cdot\hat{\mathbf{J}}(\mathbf{x})d\mathbf{x}\,,
\end{aligned} \tag{2.10}$$

where the nuclear electromagnetic current operator is[11]

$$\hat{J}_\mu=(\hat{\mathbf{J}}(\mathbf{x}),i\hat{\rho}(\mathbf{x}))\,, \tag{2.11}$$

and $\mathfrak{Y}_{LL1}{}^M$ are vector spherical harmonics.

What we shall do when we make our model is use the form of the cross section of Eq. (2.5), which was derived in a Lorentz-invariant way, and which has the relativistically correct kinematic factors extracted; and then use the above expressions, which are applicable to a fixed-source theory, to evaluate the transition matrix elements. We shall also evaluate the transition multipoles for a momentum transfer q^*. For a fixed-source theory there is no ambiguity; however, when the source recoils there is no unique prescription here. We use q^* because the original analysis[8] was carried out most directly in the rest frame of the final isobar. What we are doing, therefore, is evaluating the kinematic factors correctly, and neglecting recoil only in the transition matrix elements. In nuclear physics, at least, one can show that the main recoil correction is the density-of-states factor $[1+(2\epsilon/m)\sin^2(\theta/2)]^{-1}$, which we have treated correctly.[10] Such a treatment must break down at very large momentum transfers and our results there are at best qualitative. A better treatment, while greatly desirable, would be very difficult [witness the situation in the much simpler case of elastic scattering from the deuteron at large momentum transfers].

We will also, in our model, confine ourselves to the consideration of the Coulomb transition form factors. The motivation here is that it is known from nuclear physics that even very *crude* models of the transition

[9] For the special case $\frac{1}{2}^+\to\frac{1}{2}^+$, $f_c\sim(q^*)^2$ and $f_-\sim q^*(f_+=0)$.

[10] T. deForest and J. D. Walecka, Advan. Phys. 15, 1 (1966).

[11] There is an extra intrinsic magnetization contribution to the current in nuclear physics (see Ref. 10). $\mathbf{J}(\mathbf{x})=\mathbf{j}_N(\mathbf{x})+\nabla\times\boldsymbol{\mu}_N(\mathbf{x})$. $\mathbf{j}_N(\mathbf{x})$ is then the convection current density.

charge densities can give very reasonable form factors. For example, by saying the transition charge density is concentrated at the surface of the nucleus

$$\rho_{fi}(x) \propto \delta(x-R) \Rightarrow |f_c|^2 \propto [j_L(qR)]^2,$$

one can understand a great deal of the systematics of collective nuclear excitations.[10] One, of course, also wants to know what the transverse form factors look like, but, in nuclear physics at least, it is a problem of another order of magnitude[10] to construct a model which yields the correct excited states at the right energies and also describes the convection current correctly [in particular, maintains $\partial J_\mu(x)/\partial x_\mu \equiv 0$].

3. THE MODEL

We proceed to discuss a very simple-minded model of the nucleon. The two requirements of our model are that it should yield levels with correct quantum numbers at about the right energies and that it should allow us to compute the transition matrix elements of the charge-density operator.

We start from the following pair of observations:

(i) From a dispersion-theory point of view, the higher nucleon isobars are very complicated combinations of many-meson states. We might get a first approximation here by going to the other limit and treating the pion field as a classical field, an approximation which should be good when there are many (free) quanta present.

(ii) There should be excitations that correspond to normal-mode oscillations of the pion cloud—similar in spirit to the collective shape oscillations one has in nuclear physics.[10]

Let us start from the following Hamiltonian for a symmetric, pseudoscalar meson field[12]:

$$H=\frac{1}{2}\int d\mathbf{x}(\dot\phi_\alpha\dot\phi_\alpha+\nabla\phi_\alpha\cdot\nabla\phi_\alpha+\mu^2\phi_\alpha\phi_\alpha) +\tfrac{1}{4}\lambda\int d\mathbf{x}(\phi_\alpha\phi_\alpha)^2-\tfrac{1}{2}\beta\int_0^a d\mathbf{x}\,\phi_\alpha\phi_\alpha +\frac{G}{2m}\int d\mathbf{x}[\boldsymbol{\sigma}\cdot\nabla(\tau_\alpha\phi_\alpha)]S(x). \quad (3.1)$$

α is an isotopic-spin index which runs from 1 to 3, $S(x)$ is the nucleon source distribution function, and λ, β, and G are coupling constants. In addition to the usual pseudoscalar coupling to the nucleon source, we have included a repulsive $\frac{1}{4}\lambda(\phi_\alpha\phi_\alpha)^2$ meson-meson interaction ($\lambda>0$) for a reason which will become apparent shortly, and since (as we shall see) in our classical field theory the scattering effects of the nucleon source can essentially be transformed away, we have included a phenomenological *attractive* ($\beta>0$) potential term which scatters the meson

[12] W. Pauli, *Meson Theory of Nuclear Forces* (Interscience Publishers, Inc., New York, 1946).

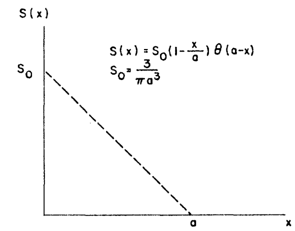

FIG. 3. Assumed form of $S(x)$, the nucleon source distribution.

when it is inside the source region. This term is meant to represent other meson exchanges with the nucleon source (ρ, f^0, etc.), baryon pair exchange, and anything else that contributes. We do not give an explicit mechanism for it here. To simplify the problem still further, we assume that S has a uniform gradient out to radius a, as shown in Fig. 3. Thus we write

$$S=\frac{3}{\pi a^3}\left(1-\frac{x}{a}\right)\theta(a-x) \quad (3.2)$$

and, partially integrating, we find

$$H_{\text{source}}=\frac{G}{2m}\int[\boldsymbol{\sigma}\cdot\nabla(\tau_\alpha\phi_\alpha)]S(x)d\mathbf{x} =\left(\frac{3g}{4\pi a^3}\right)\int_0^a \boldsymbol{\sigma}\cdot\hat{x}(\tau_\alpha\phi_\alpha)d\mathbf{x}, \quad (3.3)$$

where we have defined

$$g\equiv 4G/2ma. \quad (3.4)$$

Our starting Hamiltonian is therefore

$$H=\frac{1}{2}\int d\mathbf{x}(\dot\phi_\alpha\dot\phi_\alpha+\nabla\phi_\alpha\cdot\nabla\phi_\alpha+\mu^2\phi_\alpha\phi_\alpha) +\tfrac{1}{4}\lambda\int d\mathbf{x}(\phi_\alpha\phi_\alpha)^2-\tfrac{1}{2}\beta\int_0^a d\mathbf{x}\,\phi_\alpha\phi_\alpha +\frac{3g}{4\pi a^3}\int_0^a \boldsymbol{\sigma}\cdot\hat{x}(\tau_\alpha\phi_\alpha)d\mathbf{x}. \quad (3.5)$$

Let us now try and find the ground state of this Hamiltonian. It clearly possesses a minimum as a function of ϕ_α, since $\lambda>0$. To find the minimum we set

$$\dot\phi_0^\alpha=0, \quad (3.6)$$

which lowers the energy, and then look for vanishing variations of H:

$$\delta H/\delta\phi_0^\alpha=0. \quad (3.7)$$

This leads to the following nonlinear differential equation for the ground-state field:

$$\begin{aligned}&[\nabla^2-\mu^2-\lambda\phi_0^\beta\phi_0^\beta+\beta]\phi_0^\alpha(\mathbf{x})=\frac{3g}{4\pi a^3}\tau^\alpha(\boldsymbol{\sigma}\cdot\hat{x}), && x<a\\ &[\nabla^2-\mu^2-\lambda\phi_0^\beta\phi_0^\beta]\phi_0^\alpha(\mathbf{x})=0, && x>a\end{aligned} \quad (3.8)$$

and using this differential equation back in the Hamiltonian, we obtain

$$E_0=-\tfrac{1}{4}\lambda\int d\mathbf{x}(\phi_0{}^\alpha\phi_0{}^\alpha)^2+\frac{1}{2}\left(\frac{3g}{4\pi a^3}\right)\times\int_0^a \boldsymbol{\sigma}\cdot\hat{x}(\tau^\alpha\phi_0{}^\alpha)d\mathbf{x}. \quad (3.9)$$

We shall now look for a solution to our equations for $\phi_0{}^\alpha(\mathbf{x})$ of the form

$$\phi_0{}^\alpha(\mathbf{x})=\tau^\alpha(\boldsymbol{\sigma}\cdot\hat{x})\phi_0(x). \quad (3.10)$$

We assume that we can treat both $\boldsymbol{\sigma}$ and $\boldsymbol{\tau}$ simply as fixed vectors characterizing the nucleon source. Thus we assume that[12]

$$\frac{d}{dt}\boldsymbol{\sigma}\cong 0,\qquad \frac{d}{dt}\boldsymbol{\tau}\cong 0, \quad (3.11)$$

in our model. We want to look for normal modes of excitation that correspond to the oscillations of the existing pion cloud. The nucleon source simply serves to fix the center of mass of our system, and $\boldsymbol{\tau}$ and $\boldsymbol{\sigma}$ are included in our Hamiltonian only so that we can treat ϕ_α as a symmetric pseudoscalar meson field. Inserting this form for $\phi_0{}^\alpha(\mathbf{x})$ and using

$$\begin{gathered}\nabla^2(\boldsymbol{\sigma}\cdot\hat{x}\phi_0(x))=(\boldsymbol{\sigma}\cdot\hat{x})\left[\frac{1}{x}\frac{\partial^2}{\partial x^2}x-\frac{2}{x^2}\right]\phi_0(x),\\ (\boldsymbol{\sigma}\cdot\hat{x})^2=1,\\ \tau^\alpha\tau^\alpha=3,\end{gathered} \quad (3.12)$$

we arrive at

$$\begin{aligned}&\left[\frac{1}{x}\frac{d^2}{dx^2}x-\frac{2}{x^2}-\mu^2-3\lambda\phi_0{}^2(x)+\beta\right]\phi_0(x)=\frac{3g}{4\pi a^3}, && x<a\\ &\left[\frac{1}{x}\frac{d^2}{dx^2}x-\frac{2}{x^2}-\mu^2-3\lambda\phi_0{}^2(x)\right]\phi_0(x)=0, && x>a.\end{aligned} \quad (3.13)$$

We will return to the solution of these equations shortly. Let us assume for the moment, however, that we have the solution, and let us now look for small oscillations of the meson field about the equilibrium value. We write

$$\phi^\alpha(\mathbf{x},t)=\phi_0{}^\alpha(\mathbf{x})+\eta^\alpha(\mathbf{x},t) \quad (3.14)$$

and insert this in H. Using the differential equation satisfied by $\phi_0{}^\alpha(\mathbf{x})$, we find after a little algebra

$$\begin{aligned}H-E_0=&\frac{1}{2}\int d\mathbf{x}(\dot\eta^\alpha\dot\eta^\alpha+\nabla\eta^\alpha\cdot\nabla\eta^\alpha+\mu^2\eta^\alpha\eta^\alpha)\\ &-\tfrac{1}{2}\beta\int_0^a d\mathbf{x}\,\eta^\alpha\eta^\alpha+\tfrac{1}{4}\lambda\int d\mathbf{x}[2(\phi_0{}^\beta\phi_0{}^\beta)\eta^\alpha\eta^\alpha\\ &+4(\eta^\alpha\phi_0{}^\alpha)(\eta^\beta\phi_0{}^\beta)].\end{aligned} \quad (3.15)$$

The source term in this simple model, just as in the neutral scalar theory, has disappeared, and we are left with just the Klein-Gordon Hamiltonian for a meson field in a potential. Now using our form for $\phi_0{}^\alpha(\mathbf{x})$ and

$$\tau^\alpha\tau^\beta=\delta^{\alpha\beta}+i\epsilon_{\alpha\beta\gamma}\tau^\gamma, \quad (3.16)$$

we can reduce the Hamiltonian to[13]

$$\begin{aligned}H-E_0=&\frac{1}{2}\int d\mathbf{x}(\dot\eta^\alpha\dot\eta^\alpha+\nabla\eta^\alpha\cdot\nabla\eta^\alpha+\mu^2\eta^\alpha\eta^\alpha)\\ &-\tfrac{1}{2}\beta\int_0^a d\mathbf{x}\,\eta^\alpha\eta^\alpha+\tfrac{5}{2}\lambda\int d\mathbf{x}\,\phi_0{}^2(x)\eta^\alpha\eta^\alpha.\end{aligned} \quad (3.17)$$

The corresponding Klein-Gordon equation is

$$\begin{aligned}&\left[\nabla^2-\frac{\partial^2}{\partial t^2}-\mu^2+\beta-5\lambda\phi_0{}^2(x)\right]\eta^\alpha=0, && x<a\\ &\left[\nabla^2-\frac{\partial^2}{\partial t^2}-\mu^2-5\lambda\phi_0{}^2(x)\right]\eta^\alpha=0. && x>a\end{aligned} \quad (3.18)$$

We can look for the normal-mode solutions

$$\eta^\alpha=\eta^\alpha(\mathbf{x})e^{-i\omega t} \quad (3.19)$$

and, defining

$$\omega^2-\mu^2=k^2, \quad (3.20)$$

we finally find

$$\begin{aligned}&[\nabla^2+k^2-v(x)]\eta^\alpha(\mathbf{x})=0,\\ &v(x)=-\beta+5\lambda\phi_0{}^2(x)\quad x<a\\ &=5\lambda\phi_0{}^2(x).\quad x>a\end{aligned} \quad (3.21)$$

The problem is reduced to solving a "Schrödinger equation" in a square-well potential of depth β and range a with an additional repulsive potential $5\lambda\phi_0{}^2(x)$ coming from the presence of the ground-state meson field.[14] The reason for making this potential repulsive is now clear. It will serve to boost the centrifugal barrier and allow us to have sharp resonances high in the continuum. Let us suppose we have found the solutions to this equation, $\eta_{nlm}(\mathbf{x})$, corresponding to frequencies ω_{nl}, and normalized to

$$\int\eta_{nlm}{}^\dagger(\mathbf{x})\eta_{n'l'm'}(\mathbf{x})d\mathbf{x}=\delta_{nn'}\delta_{ll'}\delta_{mm'}. \quad (3.22)$$

We now expand the field η^α, in a fashion entirely analogous to that of the free-meson field,

$$\eta^\alpha(\mathbf{x},t)=\sum_{nlm}\frac{1}{(2\omega_{nl})^{1/2}}[c_{nlm}{}^\alpha\eta_{nlm}(\mathbf{x})e^{-i\omega_{nl}t}+c_{nlm}{}^{\alpha\dagger}\eta_{nlm}{}^\dagger(\mathbf{x})e^{i\omega_{nl}t}], \quad (3.23)$$

[13] We assume here that $[\eta^\alpha(x),\eta^\beta(x')]=0$ if $\alpha\neq\beta$. We will verify that our final solution satisfies this.

[14] This approach was first used in another context by L. I. Schiff [Phys. Rev. 84, 1 (1951)]. See also D. Yennie [Phys. Rev. 88, 527 (1952)] for a criticism of treating a $\lambda\phi^4$ theory as a classical field theory when λ or ϕ are large. He points out that quantum fluctuations then become large. We will return to this interesting point later.

and inserting this expression into the Hamiltonian, we find, after a little algebra and the use of the defining differential equations,

$$\hat{H}=E_0+\sum_{nlm\alpha}\omega_{nl}\tfrac{1}{2}[c_{nlm}{}^{\alpha\dagger}c_{nlm}{}^{\alpha}+c_{nlm}{}^{\alpha}c_{nlm}{}^{\alpha\dagger}]. \quad (3.24)$$

We can therefore immediately interpret $c_{nlm}{}^{\alpha\dagger}$ and $c_{nlm}{}^{\alpha}$ as the creation and destruction operators for these normal-mode excitations of the meson field in the presence of the ground-state meson "soup." To quantize these excitations we impose the commutation rules

$$[c_{nlm}{}^{\alpha},c_{n'l'm'}{}^{\alpha'\dagger}]=\delta_{\alpha\alpha'}\delta_{nn'}\delta_{ll'}\delta_{mm'}. \quad (3.25)$$

Let us turn our attention to the charge-density operator. We will concentrate on that part of the charge density coming from the pion field. For a Klein-Gordon field it is well known that

$$\rho(\mathbf{x},t)=\left[\phi\times\frac{\partial\phi}{\partial t}\right]_3=\epsilon_{\alpha\beta3}\phi_\alpha(\mathbf{x},t)\frac{\partial}{\partial t}\phi_\beta(\mathbf{x},t). \quad (3.26)$$

Inserting our expression for ϕ^α,

$$\phi^\alpha(\mathbf{x},t)=\phi_0{}^\alpha(\mathbf{x})+\eta^\alpha(\mathbf{x},t), \quad (3.27)$$

where η^α is the small oscillation we have

$$\rho\cong\epsilon_{\alpha\beta3}\phi_0{}^\alpha(\mathbf{x})\frac{\partial}{\partial t}\eta^\beta(\mathbf{x},t), \quad (3.28)$$

and we see that $\hat{\rho}$ is linear in the creation and destruction operators for the excitation of the meson cloud. Inserting our expression for $\phi_0{}^\alpha$ and η^β we find

$$\hat{\rho}(\mathbf{x},t)=i\epsilon_{\alpha\beta3}\tau^\alpha(\boldsymbol{\sigma}\cdot\hat{x})\phi_0(x)\times\sum_{nlm}\left(\frac{\omega_{nl}}{2}\right)^{1/2}[c_{nlm}{}^{\beta\dagger}\eta_{nlm}{}^\dagger(\mathbf{x})e^{i\omega_{nl}t}-c_{nlm}{}^{\beta}\eta_{nlm}(\mathbf{x})e^{-i\omega_{nl}t}]. \quad (3.29)$$

Going over to spherical tensor notation using[15]

$$[\mathbf{a}\times\mathbf{b}]_3=-\sqrt{2}i\sum_{qq'}(1q1q'|1110)a_{1q}b_{1q'}, \quad (3.30)$$

where a and b are tensor operators, we find

$$\hat{\rho}(\mathbf{x},t)=\sqrt{2}(\boldsymbol{\sigma}\cdot\hat{x})\phi_0(x)\sum_{qq'}\sum_{nlm}(1q1q'|1110)\tau_{1q}\left(\frac{\omega_{nl}}{2}\right)^{1/2}\times[c_{nlm,q'}{}^\dagger\eta_{nlm}{}^\dagger(\mathbf{x})e^{i\omega_{nl}t}-(-1)^{q'}c_{nlm,-q'}\eta_{nlm}(\mathbf{x})e^{-i\omega_{nl}t}]. \quad (3.31)$$

The spherical creation and destruction operators satisfy

$$[c_{nlm,q},c_{n'l'm',q'}{}^\dagger]=\delta_{nn'}\delta_{ll'}\delta_{mm'}\delta_{qq'}. \quad (3.32)$$

[15] We use the angular momentum notation of A. R. Edmonds [*Angular Momentum in Quantum Mechanics* (Princeton University Press, Princeton, New Jersey, 1957)].

The next task is to construct the states of the theory and this is very simple. The ground state is

$$|G\rangle=|0\rangle\xi_{m_s}\zeta_{m_t}, \quad (3.33)$$

where ξ_{m_s} and ζ_{m_t} are two-component spin and isospin Pauli spinors for the nucleon core, and $|0\rangle$ is the "vacuum" for the meson-field excitations:

$$c_{nlm,q}|0\rangle=0. \quad (3.34)$$

The ground state is just the nucleon with its surrounding static meson field. For an excited state of the nucleon we can now write

$$|n(l\tfrac{1}{2})JM_JTM_T\rangle=\sum_{qq'}\sum_{mm'}(1q\tfrac{1}{2}q'|1\tfrac{1}{2}TM_T)\times(lm\tfrac{1}{2}m'|l\tfrac{1}{2}JM_J)c_{nlm,q}{}^\dagger|0\rangle\xi_{m'}\zeta_{q'}. \quad (3.35)$$

We have coupled the orbital angular momentum of the meson field to the spin $\frac{1}{2}$ of the nucleon core to give a state of definite J, and the isospin 1 of the meson field to the isospin $\frac{1}{2}$ of the core to give a state of definite T. Note that these excitations have

$$T=\tfrac{1}{2},\tfrac{3}{2}\quad\text{(isospin of excitations)}.$$

The parity of these states is easily discussed. In the space of creation and destruction operators for the normal-mode excitations the parity operator is clearly given by

$$\hat{\Pi}c_{nlm}{}^{\alpha\dagger}\hat{\Pi}^{-1}=(-1)^{l+1}c_{nlm}{}^{\alpha\dagger}, \quad (3.36)$$

the extra (-1) coming from the pseudoscalarity of the pion field. This guarantees that

$$\hat{\Pi}\hat{\eta}^\alpha(\mathbf{x},t)\hat{\Pi}^{-1}=-\hat{\eta}^\alpha(-\mathbf{x},t), \quad (3.37)$$

and also gives us

$$\hat{\Pi}\hat{\rho}(\mathbf{x},t)\hat{\Pi}^{-1}=+\hat{\rho}(-\mathbf{x},t), \quad (3.38)$$

as should be so. Thus we conclude that the parity of the excited states is

$$\hat{\Pi}c_{nlm}{}^{\alpha\dagger}|0\rangle=(-1)^{l+1}c_{nlm}{}^{\alpha\dagger}|0\rangle \quad (3.39)$$

or

$$\Pi=(-1)^{l+1}\quad\text{(parity of excitations)}. \quad (3.40)$$

We have used $\hat{\Pi}|0\rangle=|0\rangle$, as must be true, since the nucleon has positive parity.

We are now in a position to compute the allowed transition matrix elements of the charge-density operator. We need

$$\langle n(l\tfrac{1}{2})JM_JTM_T|\hat{\rho}(\mathbf{x})|\tfrac{1}{2}m_s,\tfrac{1}{2}m_t\rangle=\sum_{qq'q''}\sum_{mm'}\sqrt{2}\phi_0(x)[\xi_{m'}{}^\dagger(\boldsymbol{\sigma}\cdot\hat{x})\xi_{m_s}][\zeta_{q'}{}^\dagger\tau_{q''}\zeta_{m_t}]\times(1q\tfrac{1}{2}q'|1\tfrac{1}{2}TM_T)(lm\tfrac{1}{2}m'|l\tfrac{1}{2}JM_J)\times(1q''1q|1110)\left(\frac{\omega_{nl}}{2}\right)^{1/2}R_{nl}{}^\dagger(x)Y_{lm}{}^\dagger(\Omega_x), \quad (3.41)$$

where we have written

$$\eta_{nlm}(\mathbf{x})=R_{nl}(x)Y_{lm}(\Omega_x). \tag{3.42}$$

Now let us use

$$\xi_{m'}{}^{\dagger}(\boldsymbol{\sigma}\cdot\hat{x})\xi_{m_s}=-(4\pi)^{1/2}\sum_{m''}(1m''\tfrac{1}{2}m'|1\tfrac{1}{2}\,\tfrac{1}{2}m_s)Y_{1m''}(\Omega_x)\,,\;\zeta_{q'}{}^{\dagger}\tau_{1q''}\zeta_{m_t}=\sqrt{3}(\tfrac{1}{2}m_t1q''|\tfrac{1}{2}1\tfrac{1}{2}q')\,, \tag{3.43}$$

and project out the LMth multipole:

$$\hat{M}_{LM}{}^{\mathrm{Coul}}(q^*)=\int d\mathbf{x}\,j_L(q^*x)Y_{LM}(\Omega_x)\hat{\rho}(\mathbf{x})\,, \tag{3.44}$$

using

$$\int Y_{lm}{}^*(\Omega_x)Y_{1m''}(\Omega_x)Y_{LM}(\Omega_x)d\Omega_x=(-1)^m\left[\frac{(2L+1)(3)(2l+1)}{4\pi}\right]^{1/2}\begin{pmatrix}L & l & 1\\ 0 & 0 & 0\end{pmatrix}\begin{pmatrix}L & l & 1\\ M & -m & m''\end{pmatrix}. \tag{3.45}$$

We find

$$\langle n(l\tfrac{1}{2})JM_JTM_T|\hat{M}_{LM}{}^{\mathrm{Coul}}(q^*)|\tfrac{1}{2}{}^+m_s,\tfrac{1}{2}m_t\rangle$$

$$=-(\sqrt{6})\left(\frac{\omega_{nl}}{2}\right)^{1/2}[(2L+1)(3)(2l+1)]^{1/2}\sum_{mm'm''}\sum_{qq'q''}\begin{pmatrix}L & l & 1\\ 0 & 0 & 0\end{pmatrix}\begin{pmatrix}L & l & 1\\ M & -m & m''\end{pmatrix}(-1)^m(1m''\tfrac{1}{2}m'|1\tfrac{1}{2}\,\tfrac{1}{2}m_s)$$

$$\times(\tfrac{1}{2}m_t1q''|\tfrac{1}{2}1\tfrac{1}{2}q')(1q\tfrac{1}{2}q'|1\tfrac{1}{2}TM_T)(lm\tfrac{1}{2}m'|l\tfrac{1}{2}JM_J)(1q''1q|1110)\left(\int R_{nl}{}^{\dagger}(x)j_L(q^*x)\phi_0(x)x^2dx\right), \tag{3.46}$$

and using standard angular-momentum recoupling techniques[15] we find

$$\langle n(l\tfrac{1}{2})JM_JTM_T|\hat{M}_{LM}{}^{\mathrm{Coul}}(q^*)|\tfrac{1}{2}{}^+m_s,\tfrac{1}{2}m_t\rangle$$

$$=+\left(\frac{\omega_{nl}}{2}\right)^{1/2}\left(\int R_{nl}{}^{\dagger}(x)j_L(q^*x)\phi_0(x)x^2dx\right)[(2L+1)(3)(2l+1)]^{1/2}\begin{pmatrix}L & l & 1\\ 0 & 0 & 0\end{pmatrix}(2J+1)^{1/2}\begin{Bmatrix}\frac{1}{2} & 1 & \frac{1}{2}\\ l & J & L\end{Bmatrix}$$

$$\times(-1)^{M+1}(L-MJM_J|LJ\tfrac{1}{2}m_s)3[2(2T+1)]^{1/2}\begin{Bmatrix}1 & 1 & 1\\ \frac{1}{2} & T & \frac{1}{2}\end{Bmatrix}(10TM_T|1T\tfrac{1}{2}M_T). \tag{3.47}$$

Reading off the reduced matrix element we conclude

$$\frac{4\pi}{2}|\langle n(l\tfrac{1}{2})JTM_T\|\hat{M}_L{}^{\mathrm{Coul}}(q^*)\|\tfrac{1}{2}{}^+\tfrac{1}{2}m_t\rangle|^2$$

$$=27(4\pi)(2T+1)[(2L+1)(2l+1)(2J+1)]\begin{pmatrix}L & l & 1\\ 0 & 0 & 0\end{pmatrix}^2\begin{Bmatrix}\frac{1}{2} & 1 & \frac{1}{2}\\ l & J & L\end{Bmatrix}^2\begin{Bmatrix}\frac{1}{2} & 1 & \frac{1}{2}\\ 1 & T & 1\end{Bmatrix}^2(10TM_T|1T\tfrac{1}{2}M_T)^2$$

$$\times\omega_{nl}\left|\int R_{nl}{}^{\dagger}(x)j_L(q^*x)\phi_0(x)x^2dx\right|^2 \tag{3.48}$$

This is our main result. Note that all the selection rules are contained in the 3-j and 6-j coefficients

$$\begin{aligned}&\text{(i)}\quad L+l+1\quad\text{even}\quad\text{(parity)},\\ &\qquad L=l\pm1\,,\\ &\text{(ii)}\quad L=J\pm\tfrac{1}{2}\,,\\ &\qquad J=l\pm\tfrac{1}{2}\,,\\ &\text{(iii)}\quad T=\tfrac{1}{2}\,,\tfrac{3}{2}\,.\end{aligned} \tag{3.49}$$

Now we might hope to get still more information by using our model to describe *elastic* scattering, but a very interesting thing happens. If we try and compute the contribution of the pion cloud to elastic scattering, we need

$$\hat{\rho}=\left[\boldsymbol{\phi}\times\frac{\partial\boldsymbol{\phi}}{\partial t}\right]_3\cong\left[\boldsymbol{\phi}_0\times\frac{\partial\boldsymbol{\phi}_0}{\partial t}\right]_3+\left[\boldsymbol{\phi}_0\times\frac{\partial\boldsymbol{\eta}}{\partial t}\right]_3. \tag{3.50}$$

The second term does not contribute to elastic scattering since it is linear in the creation and destruction operators, and the first term vanishes since $\partial\boldsymbol{\phi}_0/\partial t=0$. Therefore $\langle 0|\hat{\rho}|0\rangle=0$ and the meson field does not contribute to elastic scattering in this approximation. Actually this is not so unreasonable, since it is known that the elastic form factors come mainly from vector-meson exchange, and this is presumably a phenomenon relegated to our core region, as indicated in Fig. 4. However, we clearly have to be more careful, and in particular we have to worry about over-all charge conservation. Let us examine the total charge-density operator in a little more detail, including a contribution now from the nucleon source region. Let us assume

$$\hat{\rho}(\mathbf{x})\equiv s(x)\tfrac{1}{2}(1+\tau_3)+\left[\boldsymbol{\phi}\times\frac{\partial\boldsymbol{\phi}}{\partial t}\right]_3$$

$$=s(x)\tfrac{1}{2}(1+\tau_3)+\left[\boldsymbol{\phi}_0\times\frac{\partial\boldsymbol{\eta}}{\partial t}\right]_3+\left[\boldsymbol{\eta}\times\frac{\partial\boldsymbol{\eta}}{\partial t}\right]_3 \quad (3.51)$$

and we identify

$$\hat{Q}\equiv\int\hat{\rho}(\mathbf{x})d\mathbf{x}. \quad (3.52)$$

If we now insert our expressions for $\boldsymbol{\eta}$, $\boldsymbol{\phi}_0$, and $S(x)$, we see that

$$\hat{Q}=\tfrac{1}{2}(1+\tau_3)-i\sum_{nlm\alpha\beta}\epsilon_{\alpha\beta3}c_{nlm}{}^{\alpha\dagger}c_{nlm}{}^{\beta}+\int d\mathbf{x}\left[\boldsymbol{\phi}_0\times\frac{\partial\boldsymbol{\eta}}{\partial t}\right]_3. \quad (3.53)$$

The first two terms are fine, since the total isospin operator in this theory is

$$T_k\equiv\tfrac{1}{2}\tau_k+\int d\mathbf{x}\left[\boldsymbol{\eta}\times\frac{\partial\boldsymbol{\eta}}{\partial t}\right]_k$$

$$=\tfrac{1}{2}\tau_k-i\sum_{nlm\alpha\beta}\epsilon_{\alpha\beta k}c_{nlm}{}^{\alpha\dagger}c_{nlm}{}^{\beta}. \quad (3.54)$$

Unfortunately, the last term, even though it has no diagonal matrix elements, does not quite vanish, since

$$\int d\mathbf{x}\left[\boldsymbol{\phi}_0\times\frac{\partial\boldsymbol{\eta}}{\partial t}\right]_3$$

$$=i\left(\frac{4\pi}{3}\right)^{1/2}\sum_{\substack{nm\alpha\beta\\(l=1)}}\epsilon_{\alpha\beta3}\tau^{\alpha}\left(\frac{\omega_{n1}}{2}\right)^{1/2}\left\{\left(\int R_{n1}{}^{\dagger}(x)\phi_0(x)x^2dx\right)\times c_{n1m}{}^{\beta\dagger}\sigma_{1-m}(-1)^m-\text{H.c.}\right\}. \quad (3.55)$$

Note that *none* of our previous results are affected by this, since it is only the Coulomb monopole moment where we have a problem. That a problem exists is also seen if we attempt to apply Eq. (3.48) to the monopole transition $\frac{1}{2}^+\rightarrow n(1\frac{1}{2})\frac{1}{2}^+$, since we know that in the long-wavelength limit the Coulomb monopole operator is just the total charge:

$$\hat{M}_0{}^{\text{Coul}}(q^*)=\int d\mathbf{x}\; j_0(q^*x)Y_{00}(\Omega_x)\hat{\rho}(\mathbf{x})\xrightarrow[q^*\rightarrow0]{}\frac{\hat{Q}}{(4\pi)^{1/2}}, \quad (3.56)$$

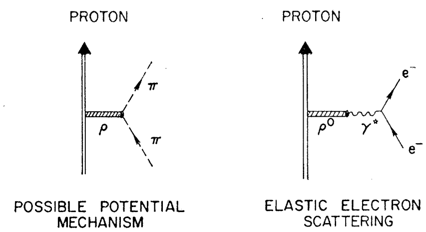

FIG. 4. Vector-meson exchange as contributing to the potential characterized by β and to elastic electron scattering.

and this operator cannot cause any transitions. Therefore the monopole matrix elements must start as q^{*2}, and Eq. (3.48) does not satisfy this requirement. We can remedy the situation in the following manner: Let us modify the charge-density operator by taking

$$\hat{\rho}(\mathbf{x})\equiv\tfrac{1}{2}(1+\tau_3)S(x)+\left[\boldsymbol{\phi}_0\times\frac{\partial\boldsymbol{\eta}}{\partial t}\right]_3+\left[\boldsymbol{\eta}\times\frac{\partial\boldsymbol{\eta}}{\partial t}\right]_3-\frac{3}{4\pi a^3}\theta(a-x)\int d\mathbf{x}\left[\boldsymbol{\phi}_0\times\frac{\partial\boldsymbol{\eta}}{\partial t}\right]_3. \quad (3.57)$$

This is presumably a more correct result, since we now have the following properties:

(i) $$\int\hat{\rho}(\mathbf{x})d\mathbf{x}=\hat{Q}=\tfrac{1}{2}+\hat{T}_3=\tfrac{1}{2}+\tfrac{1}{2}\tau_3-i\sum_{nlm\alpha\beta}\epsilon_{\alpha\beta3}c_{nlm}{}^{\alpha\dagger}c_{nlm}{}^{\beta}, \quad (3.58)$$

which is as it should be.

(ii) Since

$$\hat{H}=E_0+\sum_{nlm\alpha}\omega_n[c_{nlm}{}^{\alpha\dagger}c_{nlm}{}^{\alpha}+c_{nlm}{}^{\alpha}c_{nlm}{}^{\alpha\dagger}], \quad (3.59)$$

we have

$$[\hat{Q},\hat{H}]=0, \quad (3.60)$$

and the total charge is now a constant of the motion.[16]

(iii) In the Coulomb monopole radial matrix elements in Eq. (3.48) we must now make the replacement

$$\int R_{nl}{}^{\dagger}(x)j_0(q^*x)\phi_0(x)x^2dx\longrightarrow\int R_{nl}{}^{\dagger}(x)\left[j_0(q^*x)-\frac{3}{q^*a}j_1(q^*a)\right]\phi_0(x)x^2dx \quad (\tfrac{1}{2}^+\rightarrow n(1\tfrac{1}{2})\tfrac{1}{2}^+), \quad (3.61)$$

[16] Notice $[\mathbf{T},\hat{H}]=0$. In the same spirit we take the angular momentum operator to be

$$\mathbf{J}\equiv\tfrac{1}{2}\boldsymbol{\sigma}-\int d\mathbf{x}\,\frac{\partial\eta^{\alpha}}{\partial t}[\mathbf{x}\times\boldsymbol{\nabla}]\eta^{\alpha}=\tfrac{1}{2}\boldsymbol{\sigma}+\sum_{nlmm'\alpha}c_{nlm'}{}^{\alpha\dagger}\langle nlm'|\mathbf{L}|nlm\rangle c_{nlm}{}^{\alpha}.$$

This $\mathbf{J}$ is now the generator of rotations, as we see from Eqs. (3.31), (3.44), and (3.45),

$$\hat{R}(\omega)\hat{M}_{LM}\hat{R}(\omega)^{-1}=\sum_{M'}\mathfrak{D}_{M'M}{}^{L}(\omega)\hat{M}_{LM'};$$

and commutes with the Hamiltonian of Eq. (3.24):

$$[\hat{H},\mathbf{J}]=0.$$

which at least has the correct threshold behavior built in.

(iv) None of our other results are affected, since these arguments only concern the monopole moment.

We are now in a position to compute *elastic* scattering in this model, and we have

$$\int e^{i\mathbf{q}^*\cdot\mathbf{x}}\langle\tfrac{1}{2}+\tfrac{1}{2}m_t|\hat{\rho}(\mathbf{x})|\tfrac{1}{2}+\tfrac{1}{2}m_t\rangle d\mathbf{x} = \zeta_{m_t}{}^\dagger[\tfrac{1}{2}(1+\tau_3)]\zeta_{m_t}\int e^{i\mathbf{q}^*\cdot\mathbf{x}}S(x)d\mathbf{x}, \quad (3.62)$$

and, therefore, we can immediately identify the isoscalar and isovector elastic-charge form factors as

$$G_E{}^S(q^*)=G_E{}^V(q^*)=\int e^{i\mathbf{q}^*\cdot\mathbf{x}}S(x)d\mathbf{x}. \quad (3.63)$$

We can evidently use these relations to completely determine the source function $S(x)$.

We proceed to a discussion of solving the equations for $\phi_0(x)$ and $\eta_{nlm}(x)$. The equation for $\phi_0(x)$ is a nonlinear differential equation which we have so far solved only in a few limiting cases. It was, however, derived from the variational principle

$$\delta H_0/\delta\phi_0{}^\alpha=0, \quad (3.64)$$

where

$$H_0=\frac{1}{2}\int d\mathbf{x}[\nabla\phi_0{}^\alpha\cdot\nabla\phi_0{}^\alpha+\mu^2\phi_0{}^\alpha\phi_0{}^\alpha]-\tfrac{1}{2}\beta\int_0^a\phi_0{}^\alpha\phi_0{}^\alpha d\mathbf{x} +\tfrac{1}{4}\lambda\int d\mathbf{x}(\phi_0{}^\alpha\phi_0{}^\alpha)^2+\frac{3g}{4\pi a^3}\int_0^a \boldsymbol{\sigma}\cdot\hat{x}(\tau^\alpha\phi_0{}^\alpha)d\mathbf{x}, \quad (3.65)$$

and we can use this principle to get an approximate solution for $\phi_0{}^\alpha$. We write

$$\phi_0{}^\alpha(\mathbf{x})=\tau^\alpha(\boldsymbol{\sigma}\cdot\hat{x})\phi_0(x) \quad (3.66)$$

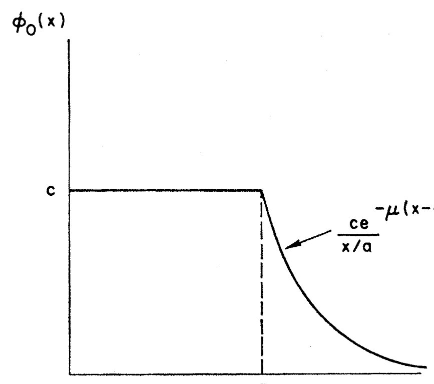

FIG. 5. Crude variational form for $\phi_0(x)$.

again, and as a variational form we take

$$\begin{aligned}\phi_0(x)&=c, & x<a\\ &=c\frac{e^{-\mu(x-a)}}{(x/a)}, & x>a\end{aligned} \quad (3.67)$$

as sketched in Fig. 5. We treat c as the parameter to be varied. Inserting this expression into H_0, we find

$$H_0=\tfrac{4}{3}\pi a^3\left[\left(\frac{9g}{4\pi a^3}\right)c+\frac{3}{2a^2}\{3(1+\mu a)+6[1+I_2(\mu a)] -\beta a^2+(\mu a)^2\}c^2+\tfrac{1}{4}9\lambda[1+3I_4(\mu a)]c^4\right], \quad (3.68)$$

where

$$I_n(\mu a)=e^{n\mu a}\int_1^\infty e^{-n\mu a t}dt/t^2,$$

and setting

$$\delta H_0/\delta c=0 \quad (3.69)$$

we find

$$\frac{9g}{4\pi a}+3\{3(1+\mu a)+6[1+I_2(\mu a)]-\beta a^2+(\mu a)^2\}c +9\lambda a^2[1+3I_4(\mu a)]c^3=0. \quad (3.70)$$

Let us consider the following limiting case of this result:

$$\begin{aligned}&\beta a^2\gg 1,\\ &\mu a\approx 1,\\ &3\lambda c^2a^2\ll\beta a^2.\end{aligned} \quad (3.71)$$

This is the situation we will actually be most interested in. We find, under these conditions,

$$c\cong\left(\frac{3g}{4\pi a}\right)\frac{1}{\beta a^2} \quad \text{(variational)}. \quad (3.72)$$

The exact solution in a very similar case is given in the Appendix. If

$$\begin{aligned}&\lambda\left(\frac{3g}{4\pi}\right)^2\frac{1}{(\beta a^2)^2}\lesssim 1,\\ &\mu a\approx 1,\\ &K^2a^2\cong\beta a^2\gg 1,\\ &|(\beta a^2)^{1/2}\tan[(\beta a^2)^{1/2}]|\gg 1,\end{aligned} \quad (3.73)$$

the solution reduces to

$$\begin{aligned}\phi_0&\cong\frac{3g}{4\pi a}\frac{1}{\beta a^2}, & x<a\\ \phi_0&\cong\frac{3g}{4\pi a}\frac{1}{\beta a^2}\left(\frac{\mu a}{1+\mu a}\right)\left(\frac{1+\mu x}{\mu x}\right)\frac{e^{-\mu(x-a)}}{(x/a)}, & x>a\end{aligned} \quad (3.74)$$

and our variational solution is almost exact in this limit.

The nice thing about this variational form is that the potential which now enters into the equation for $\eta(\mathbf{x})$,

$$
\begin{aligned}
&[\nabla^2+k^2-v(x)]\eta=0\,,\\
&v(x)=-\beta+5\lambda c^2\,, \qquad x<a\\
&\quad\;\;=5\lambda c^2\frac{e^{-2\mu(x-a)}}{(x/a)^2}\,, \qquad x>a
\end{aligned}
\tag{3.75}
$$

is such a simple one. We show the situation in Fig. 6. We now make the following observations:

(i) The effective repulsive barrier for the solution inside the potential is, including the centrifugal barrier,

$$[l(l+1)+5\lambda c^2a^2]/a^2 \quad \text{(barrier height)}\,. \tag{3.76}$$

If this quantity is greater than k^2, the states will be "quasistationary" states and will show up as resonances in electron excitation. We also expect that because of the additional centrifugal barrier, only the highest-l states will show up as sharp resonances, as appears to be the case experimentally. This of course depends on the λc^2, and we must come back and check at the end that our barrier actually has the required height to be above those states which we assume to show up as resonances, and to be below those states which we assume do not.

(ii) If the barrier is sufficiently greater than k^2, we do not change the solution inside the potential by extending the barrier up to infinity. We can immediately write down the solutions in this case:

$$
\begin{aligned}
&\eta_{nlm}(\mathbf{x})=R_{nl}(x)Y_{lm}(\Omega_x)\,,\\
&R_{nl}(x)=\left(\frac{2}{a^3 j_{l+1}{}^2(X_{nl})}\right)^{1/2} j_l(K_{nl}x)\,,
\end{aligned}
\tag{3.77}
$$

where $X_{nl}\equiv K_{nl}a$ and $j_l(X_{nl})=0$. The last condition is the familiar eigenvalue equation coming from the vanishing of the solution at the boundary. We evidently have

$$k_{nl}{}^2=(1/a^2)[X_{nl}{}^2-\beta a^2+5\lambda c^2a^2]\,, \tag{3.78}$$

and since

$$\omega_{nl}{}^2=k_{nl}{}^2+\mu^2\geqslant 0\,, \tag{3.79}$$

only $k_{nl}{}^2\geqslant-\mu^2$ are meaningful and only $k_{nl}{}^2\geqslant 0$ are true continuum resonances.

TABLE I. Resonant masses for the choice of parameters in the text.

l	$[l(l+1)+5\lambda c^2a^2]/(\mu a)^2$	$(k_{1l}/\mu)^2$	$(W-m)/\mu$	$(m^2+k_{1l}{}^2)^{1/2}/\mu$
0	40			
1	42	4.1	2.6	7.0
2 $\leftrightarrow 2s$	46	17.2	5.6	8.0
3 $\leftrightarrow 2p$	52	32.8	7.9	8.8
4 $\leftrightarrow 2d$	60	51.0	10.3	9.8
5	70	71.5	12.6	10.8

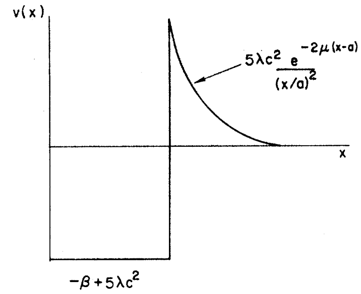

FIG. 6. The potential $v(x)$ in $[\nabla^2+k^2-v(x)]\eta=0$.

We have computed the resulting spectrum for the following choice of parameters:

$$
\begin{aligned}
&\mu a=1\,,\\
&\beta a^2-5\lambda c^2a^2=16\,,\\
&5\lambda c^2a^2=40\,.
\end{aligned}
\tag{3.80}
$$

This is not meant to be a "best fit," but is simply chosen as illustrative. This choice of parameters gives $\beta a^2\gg 1$, $\mu a\approx 1$, and $3\lambda c^2a^2\ll\beta a^2$, so that the situation discussed above is applicable. Also, with these parameters $(\beta a^2)^{1/2}\tan[(\beta a^2)^{1/2}]\approx 20$. Our variational solution should be a fair approximation in this case. We calculate the total energy in the c.m. system:

$$W=(\mathbf{k}^2+\mu^2)^{1/2}+(\mathbf{k}^2+m^2)^{1/2}\cong M\,, \tag{3.81}$$

and identify this with the mass of the resonance. The results are shown in Table I and in Fig. 7. In Table I we show the barrier height and verify that it is above the calculated eigenvalues. The places where the $2s$, $2p$, and $2d$ levels would show up in an infinite well are also indicated. We include the quantity $(m^2+k_{1l}{}^2)^{1/2}/\mu$ to get

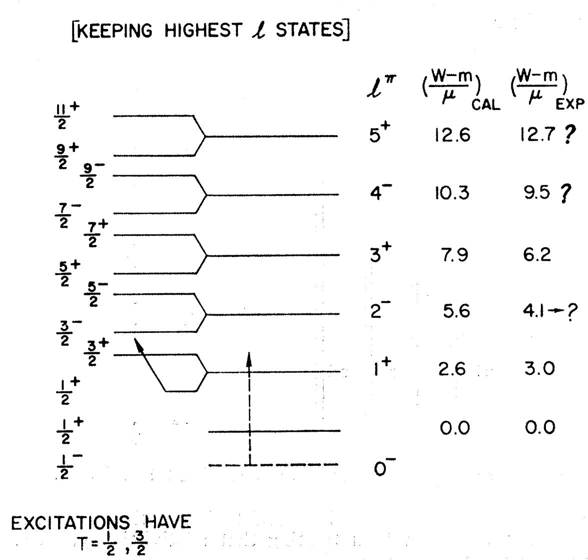

FIG. 7. Spectrum for the choice of parameters in the text: $\mu a=1$, $\beta a^2-5\lambda c^2a^2=16$.

some feel for the severity of our fixed-source approximation.[17] In Fig. 7 we show the resulting spectrum. The main features of this result are the following:

(i) Coupling the spin of the nucleon to the meson excitations, and keeping just the highest-l states as we go up in energy (as these are the states which will have a high enough barrier to show up as resonances), we get a spectrum very similar to that observed for the nucleon. The fact that $\pi=(-1)^{l+1}$, i.e., that we are dealing with a pseudoscalar field, is essential for achieving this. We assume, in Fig. 7, that there is some additional interaction which splits the $J=l\pm\frac{1}{2}$ degeneracy of our model. The quantity $(W-m/\mu)_{\exp}$ is simply taken as the average of the positions of the corresponding observed levels.

(ii) The excitations have $T=\frac{1}{2}$ and $\frac{3}{2}$, since we couple the isovector excitations to the isospin of the core. In one sense this is a success, since it restricts us to the lowest isospin states, as in the experimental case. However, it essentially gives us a doubling of the number of levels, since it appears to be quite systematic that the $J=l-\frac{1}{2}$ level has $T=\frac{1}{2}$ and the $J=l+\frac{1}{2}$ level has $T=\frac{3}{2}$. It is much less embarassing to the theory to have too many levels than not enough, though. We can easily correct the situation with a rather *ad hoc* procedure. If we define the projection operators

$$\begin{aligned} &P_{\uparrow\uparrow} \text{ projects } J=l+\tfrac{1}{2},\quad T=\tfrac{3}{2}, \\ &P_{\downarrow\downarrow} \text{ projects } J=l-\tfrac{1}{2},\quad T=\tfrac{1}{2}, \end{aligned} \tag{3.82}$$

and simply replace

$$\beta\rightarrow\beta(P_{\uparrow\uparrow}+P_{\downarrow\downarrow}), \tag{3.83}$$

we will obtain almost the correct spectrum. It is evidently too strong a statement to assume that β is independent of spin and isospin as we have done. Again, an interesting question is to find a mechanism for this form of β.[18]

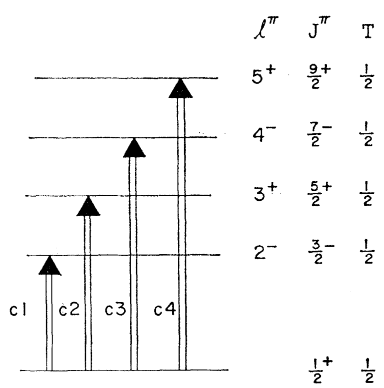

FIG. 8. The allowed normal-parity Coulomb transitions.

(iii) There is a low-lying S-wave state ($\frac{1}{2}^-$) but its exact position is, of course, very sensitive to what goes on in the inner region of the nucleon.[19] The low-lying $\frac{1}{2}^+$ state will get pushed up by its interaction with the ground state.

All in all, the model seems to give some faint reflection of the experimental situation. One can simply raise the repulsive barrier $5\lambda c^2a^2$ while keeping the depth of the well $\beta a^2-5\lambda c^2a^2$ fixed, and in this manner understand the apparent experimental continuation of the structure of Fig. 7 to higher energies. The problem then is why the $2p$, $2d$, $2f$, $3p$, etc. levels do not show up as resonances. Of course these levels would be much broader, but perhaps one needs a more sophisticated potential which is less attractive near the center of the nucleon to get rid of these states. There are, of course, also the multiquantum excitations of all the levels. These will not be excited by allowed Coulomb transitions, however.

We are now in a position to calculate $|f_c|^2$ for the allowed normal-parity Coulomb excitations. These are the transitions $\frac{1}{2}^+\rightarrow\frac{3}{2}^-, \frac{5}{2}^+, \frac{7}{2}^-\cdots(T=\frac{1}{2})$, and we show the situation in Fig. 8. They take place through the

TABLE II. The quantity X_{1l}.

l	X_{1l}
0	π
1	4.49
2	5.76
3	6.99
4	8.18
5	9.36

$C1$, $C2$, $C3$, $\cdots$ multipoles. Using our expressions for $R_{nl}(x)$ and $\phi_0(x)=c$ in the overlap region, we find

$$\begin{aligned} |f_c|^2&=\frac{4\pi}{2}|\langle(l\tfrac{1}{2})J^\pi,\tfrac{1}{2}M_T\|\hat{M}_L{}^{\mathrm{Coul}}(q^*)\|\tfrac{1}{2}^+,\tfrac{1}{2}M_T\rangle|^2 \\ &=8\pi(2L+1)(2l+1)(2J+1)\begin{pmatrix}L & l & 1\\ 0 & 0 & 0\end{pmatrix}^2\begin{Bmatrix}\frac{1}{2} & 1 & \frac{1}{2}\\ l & J & L\end{Bmatrix}^2 \\ &\quad\times(\omega_n a)(ca)^2\left(\frac{2}{j_{l+1}{}^2(X_{1l})}\right) \\ &\quad\times\left|\frac{1}{X_{1l}{}^3}\int_0^{X_{1l}} j_L(q_{1l}t)j_l(t)t^2dt\right|^2, \end{aligned} \tag{3.84}$$

for $\frac{1}{2}^+\rightarrow\frac{3}{2}^-, \frac{5}{2}^+, \frac{7}{2}^-, \frac{9}{2}^+$, etc. ($T=\frac{1}{2}$) (note that $L=l-1$ here), where we have converted the integral to dimen-

[17] The use of the Klein-Gordon Hamiltonian for the meson field means that we are at least treating that relativistically, as, of course, we must at these energies.

[18] See for example P. Carruthers, in *Lectures In Theoretical Physics* (University of Colorado Press, Boulder, Colorado, 1965), for a discussion of this problem and for further references in this area.

[19] $\frac{1}{2}^-$, $T=\frac{1}{2}$, $\frac{3}{2}$ resonances have been observed in phase-shift analyses in the region $M=1500$–1700 MeV. L. D. Roper, in *Proceedings of the Williamsburg Conference on Intermediate-Energy Physics* (William and Mary College, Williamsburg, Virginia, 1966), p. 495.

sionless variables, and

$$q_{1l} \equiv q^* a / X_{1l}. \tag{3.85}$$

We recall that X_{1l} is the first zero of the lth Bessel function. It is shown in Table II. It clearly makes more sense to look at the reduced quantity[20]

$$|f_c|^2/(\mu a)(ca)^2 \quad \text{[reduced form factor]}, \tag{3.86}$$

since this quantity, *when plotted against* q_{1l}, *no longer depends on any of the parameters of the theory.* Thus all the shapes and relative form factors are predicted in a parameter-independent fashion. The model still enters through the exact shape of the radial-wave-function overlap, but we would expect that this might be a finer detail, as is the case for Coulomb excitation of collective levels in nuclei.[10] We have plotted this quantity out to

TABLE III. CEA values of $|f_c|^2$ using the analysis of the experimental data discussed in the text.[a] [Energies and momenta in BeV.]

State	ϵ	q^2	q^*	q_0	$\xi/(1+\xi)$	$\frac{1}{2}\pi A\Gamma$ [a] (cm²)	$\lvert f_c\rvert^2$
1.512	2.358	0.795	0.917	−0.202	0.93	0.98×10^{-32}	0.080
1.512	2.988	1.31	1.145	−0.033	1.00	0.36×10^{-32}	0.049
1.512	4.874	3.29	1.92	0.623	0.85	0.69×10^{-34}	0.003
1.688	2.358	0.652	0.90	−0.388	0.78	0.89×10^{-32}	0.085
1.688	2.988	1.14	1.095	−0.242	0.94	0.33×10^{-32}	0.047
1.688	4.874	3.05	1.775	+0.322	0.96	0.78×10^{-34}	0.003

[a] Reference 6.

the first diffraction minima for the three levels

J^π	T	W_{exp} (MeV)	
$\frac{3}{2}-$	$\frac{1}{2}$	1518	(3.87)
$\frac{5}{2}+$	$\frac{1}{2}$	1688	
$\frac{7}{2}-$	$\frac{1}{2}$	2190	

in Fig. 9. The energy of the corresponding experimentally observed level is also indicated above. We compute ω_n from this number. The most interesting feature of these curves is that they have the same shape and same maximum height but they are simply displaced relative to each other, the higher multipoles having their maxima at higher q_{1l}.

4. COMPARISON WITH EXISTING EXPERIMENTAL DATA

Some recent CEA data[6] have just become available which allow us to make a comparison with this simple model. The inelastic cross sections to the $\frac{3}{2}^-$, $T=\frac{1}{2}$ (1518 MeV) and $\frac{5}{2}^+$, $T=\frac{1}{2}$ (1688 MeV) levels have been measured at 31° and incident energies $\epsilon=2.358$, 2.988, and 4.874 BeV. No experimental separation of the transverse and Coulomb contributions has yet been carried out, and we have to rely on the theory to make

[20] Note that both $|f_c|^2$ and $(\mu a)(ca)^2$ are dimensionless.

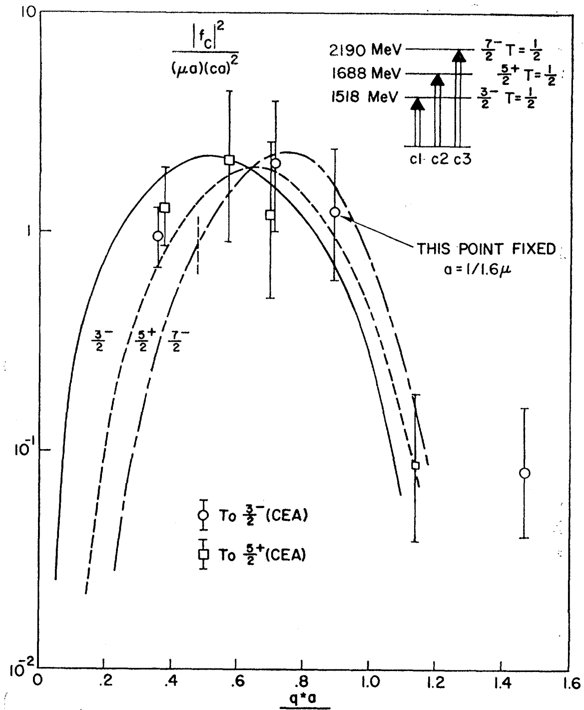

FIG. 9. The reduced form factors $|f_c|^2/(\mu a)(ca)^2$ of Eq. (3.84) plotted against the reduced momentum transfer $q_{1l}=q^*a/X_{1l}$ for the allowed normal-parity Coulomb transitions. The first zero of the lth Bessel function, X_{1l}, is given in Table II. Note $l=L+1$, where L is the Coulomb multipolarity. Also plotted is the recent CEA data (Ref. 6) analyzed as discussed in the text and summarized in Tables III and IV. The plot of the data is normalized to the indicated point as discussed in Eqs. (4.15), (4.16), and (4.17). The resulting threshold for the $\frac{1}{2}^+ \to \frac{7}{2}^-$ transition is indicated with a vertical line on the figure.

this separation. Since the experiments are at forward angles, one expects the Coulomb excitation of the collective levels (the allowed normal-parity Coulomb transitions) to dominate the cross section. Since these are normal-parity transitions, we can use the relation

$$\frac{|f_+|^2+|f_-|^2}{|f_c|^2} \underset{q^*\to 0}{\approx} \frac{J+\frac{1}{2}}{J-\frac{1}{2}}\left(\frac{q_0}{q^*}\right)^2 \tag{4.1}$$

to get an idea of the relative contributions. The indication is that under the conditions of the CEA experiments, the transverse contribution is indeed very small and the excitation of these levels is predominantly Coulomb. If ξ is the relative contribution of the Coulomb and transverse terms in the differential cross section,

$$\xi \cong \frac{J-\frac{1}{2}}{J+\frac{1}{2}}\left(\frac{q^2}{q_0^2}\right)\frac{1}{\frac{1}{2}+(q^{*2}/q^2)(M/m)^2\tan^2(\theta/2)}, \tag{4.2}$$

then the observed cross section must be multiplied by $\xi/(1+\xi)$ to get the Coulomb cross section. We give this factor in Table III, and it is almost 1 at all incident energies. Of course, the above estimate depends on a threshold condition, and is therefore crude, but in the absence of an experimental separation it is all we have to go on. The CEA group assumes a resonance shape[6]

$$\left.\frac{d^2\sigma}{d\epsilon' d\Omega}\right|_{\text{res}} = \frac{A\Gamma^2/4}{(\epsilon'-\epsilon_{\text{res}}')^2+\Gamma^2/4}, \tag{4.3}$$

which implies

$$\begin{aligned} \left.\frac{d^2\sigma}{d\epsilon' d\Omega}\right|_{\text{res peak}} &= A\,, \\ \int \left.\frac{d^2\sigma}{d\epsilon' d\Omega}\right|_{\text{res}} d\epsilon' &= \tfrac{1}{2}\pi A\Gamma \equiv \left.\frac{d\sigma}{d\Omega}\right|_{\text{lab}}, \end{aligned} \tag{4.4}$$

and they give values for $\frac{1}{2}\pi A\Gamma$, the quantities of direct relevance to the analysis here. These are shown in Table III. We can therefore find $|f_c|^2$ from the relation

$$|f_c|^2{}_{\text{exp}} = \frac{[1+(2\epsilon/m)\sin^2(\theta/2)]}{\sigma_M} \times \left(\frac{q^{*4}}{q^4}\right)\left(\frac{\xi}{1+\xi}\right)(\tfrac{1}{2}\pi A\Gamma)_{\text{exp}}, \tag{4.5}$$

where

$$\sigma_M \equiv \frac{\alpha^2\cos^2(\frac{1}{2}\theta)}{4\epsilon^2\sin^4(\frac{1}{2}\theta)} \tag{4.6}$$

and these are shown in Table III. The necessary kinematical relations are

$$\begin{aligned} &\text{(i)} && \epsilon' = \frac{\epsilon-(1/2m)[M^2-m^2]}{1+(2\epsilon/m)\sin^2(\frac{1}{2}\theta)}, \\ &\text{(ii)} && q^2 = 4\epsilon\epsilon'\sin^2(\tfrac{1}{2}\theta), \\ &\text{(iii)} && q^{*2} = q^2+(1/4M^2)[M^2-m^2-q^2]^2, \\ &\text{(iv)} && q_0 = -(1/2M)[M^2-m^2-q^2]. \end{aligned} \tag{4.7}$$

We can also get one value of $|f_c|^2$ from photoabsorption as discussed in Sec. 2. We use

$$|f_c|^2 \cong \frac{J-\frac{1}{2}}{J+\frac{1}{2}}\left(\frac{q^*}{q_0}\right)^2(|f_+|^2+|f_-|^2) \tag{4.8}$$

(if this relation is ever to work it must work here) and

$$\begin{aligned} \int_{\text{lab; over resonance}} \sigma_\gamma(\omega)d\omega &= \frac{4\pi^2\alpha}{M^2-m^2}\frac{M^2}{m}(|f_+|^2+|f_-|^2)_{q^2=0} \\ &\cong \frac{4\pi^2\alpha}{M^2-m^2}\frac{M^2}{m}\left(\frac{J+\frac{1}{2}}{J-\frac{1}{2}}\right) \\ &\quad \times(|f_c|^2)_{q^*=(M^2-m^2)/2M}. \end{aligned} \tag{4.9}$$

TABLE IV. Value of $|f_c|^2$ from photoproduction.[a]

State (BeV)	q^* (BeV)	$\frac{1}{2}\pi\Gamma m$ [a] (BeV^2)	$\sigma_\gamma(\omega_R)$ [a] (cm^2)	$\|f_c\|^2$
1.512	0.465	0.20	0.7×10^{-28}	0.038
1.688	0.580	0.21	0.6×10^{-28}	0.051

[a] Reference 6.

If we write the photoabsorption cross section

$$\sigma_\gamma(\omega) = \frac{\sigma_\gamma(\omega_R)\Gamma^2/4}{(\omega-\omega_R)^2+\Gamma^2/4}, \tag{4.10}$$

then

$$\int \sigma_\gamma(\omega)d\omega = \tfrac{1}{2}\pi\Gamma\sigma_\gamma(\omega_R). \tag{4.11}$$

The CEA group gives a value for $\sigma_\gamma(\omega_R)$ from a compilation of existing data, and to get $\frac{1}{2}\pi\Gamma$ we have used the value of

$$\int \frac{d^2\sigma}{d\epsilon' d\Omega'}d\epsilon' \Big/ \left.\frac{d^2\sigma}{d\epsilon' d\Omega'}\right|_{\text{peak}} = \tfrac{1}{2}\pi A\Gamma/A = \tfrac{1}{2}\pi\Gamma \tag{4.12}$$

given in their paper. These numbers extrapolate to the values shown in Table IV.[6] Thus we have

$$|f_c|^2{}_{q^*=(M^2-m^2)/2M} \cong \left(\frac{M^2-m^2}{4\pi^2\alpha}\right)\left(\frac{m}{M^2}\right)\left(\frac{J-\frac{1}{2}}{J+\frac{1}{2}}\right) \times(\tfrac{1}{2}\pi\Gamma)[\sigma_\gamma(\omega_R)]. \tag{4.13}$$

The values are shown in Table IV.

We now want to put these points on our reduced form factor plots in Fig. 9. To do this we have to fix both the horizontal (a) and vertical (c^2) scales. We do this by arbitrarily fitting to the point indicated in Fig. 9. Thus we take

$$\frac{|f_c|^2}{(\mu a)(ca)^2} = 1.25, \quad \frac{q^* a}{X_{12}} = 0.89 \quad \text{(from fitting)} \tag{4.14}$$

for the experimental point for $\frac{1}{2}^+ \to \frac{3}{2}^-$, $T=\frac{1}{2}$ (1518 MeV):

$$|f_c|^2 = 0.049, \quad q^* = 1.145 \text{ BeV} \quad \text{(experimental values)}. \tag{4.15}$$

This allows us to determine the constants

$$a = 1/1.6\mu, \quad (\mu a)(ca)^2 = 0.039 \quad \text{(from fitting)}. \tag{4.16}$$

The *relative positions of all the other experimental points for both levels is now completely determined.*

5. DISCUSSION

The most interesting features of the comparison in Fig. 9 are the following:

(i) From a comparison of the shapes of the theoretical and experimental form factors, the relevance of the threshold behaviors mentioned in the introduction becomes clear. These threshold behaviors can be thought of as coming from the expansion of the Bessel functions occurring in the transition multipoles:

$$j_L(qx)\approx\frac{(qx)^L}{(2L+1)!!}\leqslant\frac{(qR)^L}{(2L+1)!!} \qquad (5.1)$$

(R is the interaction radius), and these expansions require that we be on the ascending side of the form factors shown in Fig. 8. In fact, with the aid of the photoabsorption points—the points farthest to the left—we see that we are still in the ascending region with the experimentally obtainable values of q^2, although we rather quickly reach the maximum, by which point the above expansion has no relevance. We can, however, now make some predictions that we hope are meaningful about the form factors for the higher-lying states. In particular, we have now located the corresponding threshold for the $\frac{1}{2}^+\rightarrow\frac{7}{2}^-$ (2190 MeV) form factor, and we see that this form factor should increase well into the experimentally obtainable region. We are also able to predict where the maximum in this form factor should occur. These peaks should thus be clearly evident in the higher-energy scattering experiments. From just looking at the experimental points themselves, it is clear that these conclusions are not particularly model-dependent. They do, however, rely rather heavily on the values for the photoabsorption cross sections.

(ii) One very interesting prediction, which appears to be very well satisfied experimentally, is that the two form factors should achieve the same maximum value, and we can then extrapolate this value to the higher levels. This is a model-dependent prediction, since there is no *a priori* relationship between these relative transition strengths.

(iii) The fact that the relative fit to the two different levels agrees fairly well is an indication that we have approximately the same interaction radius a for these two levels. This is also a model-dependent statement, but not a very striking one, as might be expected on rather intuitive grounds. In fact, if we take the fit in Fig. 9 very seriously, there is some evidence that we should use a slightly *smaller* value of the radius for the $\frac{1}{2}^+\rightarrow\frac{3}{2}^-$ (1518 MeV) transition. If there is a strong variation of radius from level to level, then measuring the transition form factor will not be a very powerful tool for determining transition multipolarities (as it is, for example, in nuclear physics).[10] Just looking at the existing data, one is not in a very strong position as far as differentiating multipolarities is concerned.

(iv) The existence of a diffraction "decrease" at the larger values of q^2 seems rather well established.

Let us now turn our attention briefly to the empirically determined size of the parameters in the theory and to the over-all consistency of the model.

(a) We have seen that

$$a\cong 1/1.6\mu \quad \text{(empirical)}. \qquad (5.2)$$

Our rough fit to the spectrum in Fig. 6 used $a\mu=1$. These values are different; however, they are still close enough so that the model is not complete nonsense. We can get another piece of information here by using the model to describe *elastic* scattering, using Eq. (3.62). Our assumed uniform-gradient source distribution will not give a good fit to elastic scattering; however, we can at least try to fit the mean-square radius of the proton. Using the shape in Fig. 3, we compute

$$\langle r^2\rangle=\tfrac{2}{5}a^2, \qquad (5.3)$$

and using

$$\sqrt{\langle r^2\rangle_{\text{proton}}}\cong 0.8\ \text{F}, \qquad (5.4)$$

we find

$$a=1/1.1\mu, \qquad (5.5)$$

which gives a source radius only slightly larger than that of the potential in Eq. (5.2).

(b) We have also seen that

$$(\mu a)(ca)^2=0.039. \qquad (5.6)$$

This determines c and hence a certain combination of the coupling constants in our theory:

$$(ca)^2=0.062. \qquad (5.7)$$

We can compare with the experimental pion-nucleon coupling constant through the tail of the pion field. We have asymptotically

$$\phi_0{}^\alpha(\mathbf{x})\underset{x\to\infty}{\longrightarrow} c\tau^\alpha(\boldsymbol{\sigma}\cdot\hat{x})\frac{e^{-\mu(x-a)}}{x/a}, \qquad (5.8)$$

whereas the tail from the one-pion-exchange pole is

$$\phi_0{}^\alpha(\mathbf{x})\underset{x\to\infty}{\longrightarrow}\frac{\mu}{2m}\frac{G_{\pi N}}{4\pi}\tau^\alpha\boldsymbol{\sigma}\cdot\hat{x}\frac{e^{-\mu x}}{x}. \qquad (5.9)$$

Comparing these results we see that

$$G_{\pi N}{}^2/4\pi=496, \qquad (5.10)$$

whereas the known value is $G_{\pi N}{}^2/4\pi=15$. Thus

$$G_{\text{empirical}}/G_{\text{theoretical}}=5.7. \qquad (5.11)$$

The coupling constant we need seems to be too large, although the tail of the pion field is only very crudely determined in this model.

(c) We can now also ask what is the actual expansion parameter when we write

$$\phi^\alpha(\mathbf{x},t)=\phi_0{}^\alpha(\mathbf{x})+\eta^\alpha(\mathbf{x},t) \qquad (5.12)$$

and assume η^α is a "small" oscillation. If we call the dimensionless expansion parameter η, then very roughly

$$\eta^2 \approx \left(\frac{(1/2\omega_n)^{1/2}(3/4\pi a^3)^{1/2}}{c[\tau^\alpha\tau^\alpha(\boldsymbol{\sigma}\cdot\hat{x})^2]^{1/2}}\right)^2$$

$$=\frac{1}{8\pi}\left(\frac{\mu}{\omega_n}\right)\frac{1}{(\mu a)(ca)^2}\approx\frac{\mu}{\omega_n}. \quad (5.13)$$

This is not an astoundingly small number, but it is less than 1, since

$$\omega_{3/2^-}=3.4\mu,$$
$$\omega_{5/2^+}=4.2\mu, \quad (5.14)$$
$$\omega_{7/2^-}=6.4\mu.$$

The interesting thing is that our approximation of looking at the normal-mode excitations of the classical meson field gets better for the higher-lying states, as we hoped in the introduction.

(d) We have now also determined a value of λ, since we assumed that

$$5\lambda c^2a^2 \cong 40 \quad (5.15)$$

to get a high enough barrier. Now a very interesting point here is made by Yennie,[14] who discusses the neutral scalar theory and shows that one cannot treat the $\lambda\phi^4$ theory as classical, even as $G\to\infty$, if $\lambda\phi_0^2$ is large enough, because of the quantum fluctuations introduced by the zero-point oscillations of our normal-mode excitations. In fact, Yennie gives an explicit formula for the corrections that are not simply renormalizations, and hence absorbed into the renormalized coupling constants. Yennie's correction to the ground-state energy effectively multiplies the $\beta\phi_0^2$ term by a factor

$$\mathfrak{Y}=\left[1+\frac{9\lambda_0}{32\pi^2}\left(\frac{\lambda_0\phi_0^2}{K^2}\right)^2\left(\frac{5}{9}\right)^3+\cdots\right], \quad (5.16)$$

where, in our theory, we would have $K^2=-\beta+\mu^2$ and $\lambda_0=3\lambda$.[21] This term gives us a measure of the contribution of these zero-point oscillations. Now it is true that we never need to calculate E_0, since we compute $E-E_0$ directly; however, we do need ϕ_0, and Yennie shows that the correct equation for ϕ_0 comes from taking $\delta E_0/\delta\phi_0=0$. The quantum correction is large when the combination $\lambda(\lambda\phi_0^2/\beta)$ is large. If we use our original choice of parameters,

$$\mu a=1,$$
$$\beta a^2=56, \quad (5.17)$$
$$5\lambda c^2a^2=40,$$

then

$$\mathfrak{Y}=1+\frac{125\lambda}{96\pi^2}\left(\frac{1}{7}\right)^2+\cdots, \quad (5.18)$$

and since λ is not determined by the above conditions, we can make λ as small as we want by making c^2 large enough. Note that our reduced form factors are independent of any of these considerations. Our empirical fit, however, determines both a and $(ca)^2$. If we proceed and attempt to estimate $\mathfrak{Y}$ from our empirical values, we can write $\phi_0^2\approx c^2$ and

$$\mathfrak{Y}=1+\frac{125\lambda}{96\pi^2}\left(\frac{\lambda c^2a^2}{\beta a^2}\right)^2. \quad (5.19)$$

Now using

$$\beta a^2=56,$$
$$5\lambda c^2a^2=40,$$
$$(ca)^2=0.062 \quad \text{(empirical)},$$

we have

$$\mathfrak{Y}-1=0.35+\cdots, \quad (5.20)$$

which indicates that the effect of quantum fluctuations on the ground state is not negligible for this particular set of parameters. However, since the empirical value of $a=1/1.6\mu$, the radius of the attractive potential, is *smaller* than we originally assumed, we will not need nearly as high a barrier coming from λ. The problem with a smaller radius is to get all the levels down at the right energy. For this, one has to change the shape of the potential term. No attempt has yet been made to find a completely consistent set of parameters and potential shape. In any event, the effect of these quantum fluctuations is certainly contained implicitly in the empirical values of the coupling constants and radius parameter a which we determine, and it is certainly important to include their effect in any rigorous theory starting from quantized fields. There is a very interesting analogous situation that comes to mind in nuclear physics. One can make a model of collective shape oscillations by studying a quantized, oscillating liquid drop.[10] This crude model does very well on the transition form factors, primarily because they are the leading terms in the charge-density operator, being linear in the creation and destruction operators (as is the case here). However, the *elastic* scattering is only very poorly described by a uniform liquid drop of definite radius, and it is essential to consider the effect of the vacuum fluctuations of the quantized surface coordinates, a second-order effect, to begin to get anything like the right ground-state properties consistently within the model.

The question of the damage done by computing the transition matrix elements in a fixed-source theory is a much more serious one. Indeed, there is a paper by the present author[22] that shows that recoil effects in the intermediate states are very important for computing the *elastic* scattering form factors in the usual static theory of the nucleon, and that the relativistic, dispersion-theory spectral functions are quite different

[21] By separating Eqs. (3.5) and (3.17) into three equations of the type studied by Yennie, one for each isospin component, and comparing with his analysis [note also our Eqs. (3.12), (3.13), and (3.18)], we see that $\lambda_0=3\lambda$ and that we must include the extra factor of $(5/9)^3$ in the correction term here.

[22] J. D. Walecka, Nuovo Cimento 11, 821 (1959).

from those of the static theory. However, even here there is a ray of hope, because it was shown in that work that one could understand essentially the entire difference between the relativistic dispersion theory and the static theory by computing the transition matrix elements to intermediate states in the static theory but using the correct relativistic kinematics in the energy denominators. These transition matrix elements occur twice in elastic scattering. Thus one might still hope that we have not done great damage to the theory by computing the first-order transition matrix elements in a static theory.

The main improvements, beside this, that one would like to make are:

(i) Include the coupling of the nucleon core to the meson excitations, so that the transverse form factors for these higher excitations could be estimated with a little confidence.[23]

(ii) Find some mechanism for the generation of the potential scattering term, which is essential to this model, and repeat the calculation with a more realistic potential and with the vacuum-fluctuation corrections included.

(iii) Eliminate the dependence on the source density $S(x)$ by taking it from elastic scattering.

In summary, then, we have made a very simple-minded model of the nucleon which gives many of the correct levels at about the right place and which allows us to compute the transition Coulomb form factors. One can raise many objections to the model, and this paper is by no means presented as an attempt to give a basic theoretical understanding of the structure of the nucleon. In fact, in several respects the model is not even consistent, although we have tried as hard as possible to make it so. The main reason for writing the paper at the present time is, as stated in the introduction, to get some predictions in *before* the experiments are carried out, which may serve as a possible guide to experimentalists in planning new experiments and correlating data as the data accumulate. Some of the predictions, for example the shape, location, and threshold location of the reduced Coulomb form factors, are probably fairly model-independent, and they will presumably be fairly useful even in the future. Other, more model-dependent statements, such as the fact that the form factors all achieve the same maximum height, are, at the very least, intriguing.

ACKNOWLEDGMENTS

It is a pleasure to acknowledge useful and stimulating discussions with J. D. Bjorken, S. D. Drell, A. L. Fetter, W. Panofsky and the members of SLAC Group A, L. I. Schiff, and Richard Wilson.

[23] *Note added in proof.* This has been done in collaboration with P. Pritchett (to be published).

APPENDIX

In this Appendix we briefly discuss a limiting case of the solution to the nonlinear differential equation

$$\begin{aligned}\left[\frac{1}{x}\frac{d^2}{dx^2}x-\frac{2}{x^2}-\mu^2-3\lambda\phi_0^2(x)+\beta\right]\phi_0(x)&=\frac{3g}{4\pi a^3}, \quad x<a\\ \left[\frac{1}{x}\frac{d^2}{dx^2}x-\frac{2}{x^2}-\mu^2-3\lambda\phi_0^2(x)\right]\phi_0(x)&=0. \qquad x>a\end{aligned}\tag{A1}$$

Our basic assumption will be that the solution is dominated by the source term,

$$3\lambda\phi_0^3 \ll 3g/4\pi a^3, \tag{A2}$$

and we will solve

$$\begin{aligned}\left[\frac{1}{x}\frac{d^2}{dx^2}x-\frac{2}{x^2}-\mu^2+\beta\right]\phi_0(x)&=\frac{3g}{4\pi a^3}, \quad x<a\\ \left[\frac{1}{x}\frac{d^2}{dx^2}x-\frac{2}{x^2}-\mu^2\right]\phi_0(x)&=0. \qquad x>a\end{aligned}\tag{A3}$$

We write

$$\phi_0^{\text{out}}=\frac{N}{x}\left[1+\frac{1}{\mu x}\right]e^{-\mu x}, \qquad x>a \tag{A4}$$

$$\phi_0^{\text{in}}=\frac{A}{x}\left[\frac{\sin Kx}{Kx}-\cos Kx\right]+\phi_p, \quad x<a \tag{A5}$$

where

$$\left(\frac{1}{x}\frac{d^2}{dx^2}x-\frac{2}{x^2}+K^2\right)\phi_p=\frac{3g}{4\pi a^3}, \quad x<a \tag{A6}$$

$$K^2 \equiv \beta-\mu^2. \tag{A7}$$

We can write the solution in this equation as $\phi_p=u_p/x$, where

$$\begin{aligned}u_p(x)&=-\int_0^x [Kxj_1(Kx)n_1(Ky)\\ &\qquad -Kxn_1(Kx)j_1(Ky)]\left(\frac{3g}{4\pi a^3}\right)y^2dy\\ &=\frac{3g}{4\pi(Ka)^3}\left[\frac{2}{Kx}(1-\cos Kx)+Kx-2\sin Kx\right].\end{aligned}\tag{A8}$$

Now imposing the boundary conditions

$$\left.\begin{aligned}\phi_0^{\text{in}}&=\phi_0^{\text{out}},\\ (x\phi_0^{\text{in}})'&=(x\phi_0^{\text{out}})',\end{aligned}\right\} \text{ at } x=a \tag{A9}$$

we find

$$\frac{A}{Ka}=\frac{-3g}{4\pi(Ka)^4}\left\{\frac{(1+\mu a+(\mu a)^2)[(Ka)^2-2Ka\sin Ka+2(1-\cos Ka)]+(1+\mu a)[(Ka)^2(1-2\cos Ka)+2Ka\sin Ka-2(1-\cos Ka)]}{(1+\mu a+(\mu a)^2)[\sin Ka-Ka\cos Ka]+(1+\mu a)[(Ka)^2\sin Ka+Ka\cos Ka-\sin Ka]}\right\}, \quad \text{(A10)}$$

$$\frac{N}{\mu a}e^{-\mu a}=\frac{3g}{4\pi(Ka)^4}\left\{\frac{[(Ka)^2-2Ka\sin Ka+2(1-\cos Ka)][(Ka)^2\sin Ka+Ka\cos Ka-\sin Ka]-[(Ka)^2(1-2\cos Ka)+2Ka\sin Ka-2(1-\cos Ka)][\sin Ka-Ka\cos Ka]}{(1+\mu a)[(Ka)^2\sin Ka+Ka\cos Ka-\sin Ka]+(1+\mu a+(\mu a)^2)[\sin Ka-Ka\cos Ka]}\right\}. \quad \text{(A11)}$$

Let us now assume that

$$\begin{aligned}\lambda\left(\frac{3g}{4\pi}\right)^2\frac{1}{(\beta a^2)^2}&\lesssim 1,\\ \mu a&\approx 1,\\ K^2a^2\cong\beta a^2&\gg 1,\\ |(\beta a^2)^{1/2}\tan[(\beta a^2)^{1/2}]|&\gg 1.\end{aligned} \quad \text{(A12)}$$

In this case our solution reduces to

$$A\cong\frac{-3g}{4\pi(Ka)^3}\left\{\frac{1+\mu a+(\mu a)^2+(1+\mu a)(1-2\cos Ka)}{(1+\mu a)\sin Ka}\right\}=O\left(\frac{1}{(Ka)^3}\right), \quad \text{(A13)}$$

$$N\cong\frac{3ge^{\mu a}}{4\pi(Ka)^2}\left(\frac{\mu a}{1+\mu a}\right). \quad \text{(A14)}$$

The leading term in our solution for ϕ_0 therefore comes from ϕ_p, and we can write in this limit [keeping terms of order $1/(Ka)^2$]:

$$\phi_0^{\text{in}}\cong\frac{3g}{4\pi a}\frac{1}{(\beta a^2)}, \qquad x<a \quad \text{(A15)}$$

$$\phi_0^{\text{out}}\cong\frac{3g}{4\pi a}\frac{1}{(\beta a^2)}\left(\frac{\mu a}{1+\mu a}\right)\left(\frac{1+\mu x}{\mu x}\right)\frac{e^{-\mu(x-a)}}{x/a}. \qquad x>a \quad \text{(A16)}$$

Our first assumed condition guarantees that

$$3\lambda\phi_0^3\leqslant\frac{3g}{4\pi a^3}\left[\lambda\left(\frac{3g}{4\pi}\right)^2\frac{1}{(\beta a^2)^2}\right]\frac{3}{\beta a^2}\ll\frac{3g}{4\pi a^3} \quad \text{(A17)}$$

and also

$$3\lambda\phi_0^2a^2\leqslant 3\left[\lambda\left(\frac{3g}{4\pi}\right)^2\frac{1}{(\beta a^2)^2}\right]\ll\beta a^2. \quad \text{(A18)}$$

We have in addition

$$3\lambda\phi_0^2a^2\leqslant 3\left[\lambda\left(\frac{3g}{4\pi}\right)^2\frac{1}{(\beta a^2)^2}\right]\lesssim(\mu a)^2+2 \quad \text{(A19)}$$

under these conditions, so that the replacement of the Eqs. (A1) by the Eqs. (A3) is also justified in this case.